Philipp Hamberger[1,2,*]
Daniela Piccioni Koch[2]
Sokratis Sinanis[1]
Karlheinz Schaber[1]

Enlargement of Submicron Gas-Borne Particles by Heterogeneous Condensation for Energy-Efficient Aerosol Separation

To improve the efficiency of aerosol separation, a process sequence for particle enlargement by condensation of water vapor on their surface is suggested. The presented method makes use of packed columns in non-equilibrium operation to achieve supersaturation, which is required for droplet growth. Although this method is known for several years, it is not widely used in industrial processes and still needs accurate investigations for consolidation and establishment. The simulation tool AerCoDe3.0 for predicting saturation and particle growth in packed columns allows investigating the thermal energy consumption under various operation conditions. Based on the results obtained in this study, optimized arrangements of columns, which are applicable as preconditioning step for existing particle separators, are proposed.

Keywords: Aerosol separation, Energy consumption, Heterogeneous condensation, Submicron particle enlargement

Received: December 13, 2018; *revised:* June 30, 2019; *accepted:* August 16, 2019

DOI: 10.1002/ceat.201800720

Supporting Information available online

1 Introduction

The enlargement of submicron gas-borne particles by heterogeneous condensation of water in a supersaturated gas phase is a well-known method for improving aerosol separation in gas cleaning processes for more than 60 years. Particle growth by condensation facilitates inertial impaction, which is the major mechanism of dust precipitation in wet scrubbers.

The lower the particle size, the higher is the specific energy expenditure for dust separation. Holzer [1] compared various types of wet scrubbers such as Venturi scrubbers, jet scrubbers, and packed columns and found a lower limit for the specific energy expenditure (kWh $(10^3\ m^3)^{-1}$) that depends on the mean particle size. This lower limit holds if inertial impaction is the dominating separation mechanism. To overcome this limitation, especially for the separation of submicron particles, condensational growth may be applied prior to inertial impaction to reduce the energy expenditure considerably.

Different preconditioning methods for the condensational enlargement of submicron dust particles have been suggested in the literature. In the very early works of Fahnoe et al. [2] and Schauer [3], steam injection techniques were applied to achieve condensational growth and a more efficient aerosol separation. Lancaster and Strauss [4] further investigated the mechanisms of steam injection into wet scrubbers and identified particle buildup by condensation, followed by inertial impaction as the dominating mechanism for improved scrubber performance. With regard to the available steam, they concluded that the efficiency of steam usage is rather low because condensation occurs rapidly before the mixing of steam and dusty gas is accomplished.

One of the first fundamental analyses of aerosol growth by condensation was carried out by Yoshida and co-workers [5], who investigated the basic principles of heterogeneous condensation and performed measurements of droplet diameters by means of an ultramicroscopic size analysis. In a succeeding paper [6], the steam injection technique was compared with the technique of mixing saturated hot air and cold air as possible supersaturation methods for industrial exhaust gas purification. Various processes were proposed for a suitable application of both methods and the procedure of their utilization with respect to the exhaust gas conditions was presented. Both methods were recommended as preconditioning techniques for exhaust gases containing dust particles with low number concentration.

Calvert [7] pointed out that vapor condensation not only increases inertial impaction but also causes thermophoretic and diffusiophoretic precipitation of submicron dust particles.

[1]Philipp Hamberger, Dr. Sokratis Sinanis, Prof. Dr.-Ing. Karlheinz Schaber
philipp.hamberger@kit.edu
Karlsruhe Institute of Technology, Institute of Thermodynamics and Refrigeration, Engler-Bunte-Ring 21, 76131 Karlsruhe, Germany.
[2]Philipp Hamberger, Dr. Daniela Piccioni Koch
Karlsruhe Institute of Technology, Steinbuch Centre for Computing, Hermann-von-Helmholtz-Platz 1, 76344 Eggenstein-Leopoldshafen, Germany.

Johannessen et al. [8] proposed a mathematical model for predicting the deposition rates and condensational growth in a packed-column scrubber. The results matched the experimental data reasonably well. The particle growth was determined by weighing a glass fiber filter on which the droplets had been precipitated. By using saturated air at a temperature of 60 °C and cold water at 13 °C, it was found that the removal efficiency improvement by cooling and condensation processes in packed columns is only significant below a particle number concentration of 10^5 cm^{-3}. However, typical number concentrations of submicron particles in exhaust gases often exceed 10^6 cm^{-3}.

Comprehensive experimental and theoretical studies on condensation-supported particle separation have been performed by Heidenreich, Ebert, and co-workers [9–11]. They investigated particle growth in packed columns and showed that supersaturation and particle growth can also be achieved if a cold gas stream is contacted with hot water. Based on this evidence, they suggested a new process for particle enlargement with two columns, where each column is trickled with water, which is alternately colder or warmer than the gas. They demonstrated that for particle number concentrations of 10^6cm^{-3} and a temperature difference of 60 °C in the first column a dust collection efficiency up to 90 % can be reached.

Despite these promising results, the industrial applications of the described techniques for the enlargement of submicron particles are rare. One reason for this are the costs to provide the additional thermal energy or cooling capacity, which is needed for generating supersaturated gas phases. This aspect has been rarely considered up to now. The design, evaluation, and optimization of energy-efficient preconditioning processes for condensational particle enlargement require a suitable simulation tool. Such a tool, which is named AerCoDe3.0, is described in Sect. 3 and has been used in the present work to predict the evolution of droplet diameters in a sequence of packed columns.

2 Heterogeneous Nucleation and Condensation

As a necessary precondition for heterogeneous nucleation of water on gas-borne particles and subsequent condensational growth, the gas phase must become supersaturated. The saturation ratio S[1)] of water vapor in an inert carrier gas flow is defined as:

$$S = \frac{p_w}{p_{sw}(T)} \tag{1}$$

if the gas phase behaves as an ideal gas, which can be assumed with good accuracy for most gas cleaning processes. p_w is the partial pressure and $p_{sw}(T)$ means the vapor pressure of water, as a function of the temperature T. S equals the relative humidity of the gas. Before heterogeneous nucleation can take place, the saturation ratio has to exceed a critical value S_{crit}. According to the basic theory of Fletcher [12] for heterogeneous nucleation on spherical insoluble particles, S_{crit} depends on the wettability, which is defined by the contact angle between condensed liquid and particle surface and by the particle diameter. For ideal wettable particles with diameters $d > 0.1$ µm, the critical saturation ratio is rather close to $S_{crit} = 1$. Later extensions of Fletcher's theory, e.g., that by Lazardis et al. for non-uniform surfaces [13], yield similar results.

Soluble submicron particles like salt particles are able to uptake water in a humid atmosphere even at a saturation ratio lower than $S = 1$, if the deliquescence point is exceeded. Typical deliquescence points for salt particles are in a range of the relative humidity between 30 and 80 % [14]. Salt particles can uptake water until the thermodynamic equilibrium is reached. The equilibrium of droplets containing an aqueous salt solution in a humid atmosphere can be calculated by considering the Kelvin effect and the vapor pressure depression. As a result, graphs in which the saturation ratio S is plotted versus the wet particle diameter at constant values of the dry salt particle mass and temperature can be obtained. These graphs are called Köhler curves. Fig. 1 shows such a plot for NH_4Cl particles where the calculation takes into account the activity of water in a non-ideal salt solution [15].

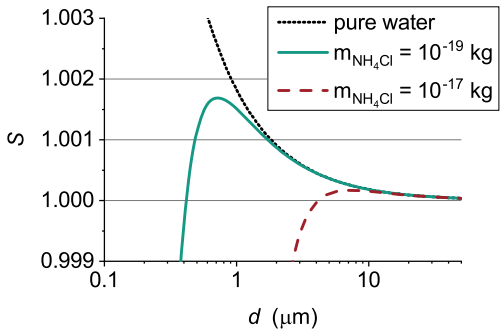

Figure 1. Equilibrium saturation ratio versus particle diameter of NH_4Cl solution droplets at 50 °C. Initial mass m_{NH4Cl} of the particles: 10^{-19} kg, corresponds to an initial diameter of 0.04 µm (solid line) and 10^{-17} kg, corresponds to an initial diameter of 0.23 µm (dashed line).

The left, steeply sloping branches of the curves represent a stable thermodynamic equilibrium. This means that dry particles or droplets can grow until this stable branch is reached. Obviously, the growth of dry soluble particles with diameters of $d < 0.1$ µm in a non-saturated atmosphere is rather limited. If particle diameters of more than 1 µm should be reached, the maximum values of the curves at saturation ratios $S > 1$ must be exceeded. Similar results were obtained for sulfuric acid and hydrochloric acid droplets [15, 16]. Consequently, for an appreciable enlargement of insoluble as well as for soluble particles up to diameters of $d > 2$ µm, at least a slight supersaturation of the surrounding gas phase is always necessary.

In principle, the precise prediction of particle growth in industrial exhaust gases based on theories for heterogeneous nucleation would require sufficient information on size distribution, surface characteristics, and wettability of the gas-borne submicron dust particles. However, such kind of data is generally not available.

1) List of symbols at the end of the paper.

For this reason, a pragmatic strategy has to be chosen for the simulation of particle growth by heterogeneous condensation. The assumption of a constant number concentration c_N of dust particles, which start to grow when the saturation exceeds the critical value S_{crit}, is made. This approach yields a monodisperse aerosol. Parametric studies with various number concentrations will give an indication on how the particle number concentration influences the final droplet diameters. It is well-known that the number concentration of submicron particles in exhaust gases typically ranges between 10^5 and 10^7 cm^{-3}.

3 Simulation Tool AerCoDe3.0

The simulation tool AerCoDe3.0 is a Fortran code for predicting saturation profiles, aerosol formation, and particle growth in gas-liquid contact devices. It is based on previous code versions developed by Körber et al. [17] and Ehrig et al. [18]. The underlying model yields a system of coupled spatially one-dimensional partial differential equations, which describe the temporal change of temperatures and compositions in the gas and liquid phases as well as in the growing aerosol droplets along the gas-liquid interface of the contact device. The present version is modified for simulations with water vapor and air as a carrier gas. Changes were made to the numerical solution of the model equations, which could be improved by implementing new integration methods.

In most cases, the stationary solution of the equation system is desired. This means that at a given point of the device, there is no change of the variables over time. Mathematically, this is expressed by setting the time derivatives to zero, which yields a system of ordinary differential equations. In general, there are no consistent initial conditions for this problem and the solution must be calculated by solving the original partial differential equations by time integration. For co-current flow columns, initial conditions for the ordinary differential equations can be defined and the solution can be calculated directly by integrating along the device interfacial area. This method is more efficient and numerically more robust. The model has been verified with experimental results in different works [19–21].

4 Simulation of Particle Enlargement in Packed-Column Sequences

AerCoDe3.0 is applied to investigate the efficiency of particle enlargement by water condensation on air-borne particles in packed columns under different operating conditions. In order to generate supersaturation as high as possible, the method, where water evaporates from hot liquid into cold gas [10], is adopted and the columns are operated in co-current flow [19]. Typical simulation results are plotted in Fig. 2.

Here, it can be observed that the curves for the gas temperature T^G and the vapor load Y_w follow each other closely (Fig. 2a). This causes supersaturation due to the exponentially increasing equilibrium vapor pressure (Fig. 2b). The simulation uses the values of Heidenreich's example [11] as input parameters: gas velocity $u^G = 2.2\,\mathrm{m\,s^{-1}}$ and gas temperature $T^G = 10\,°C$.

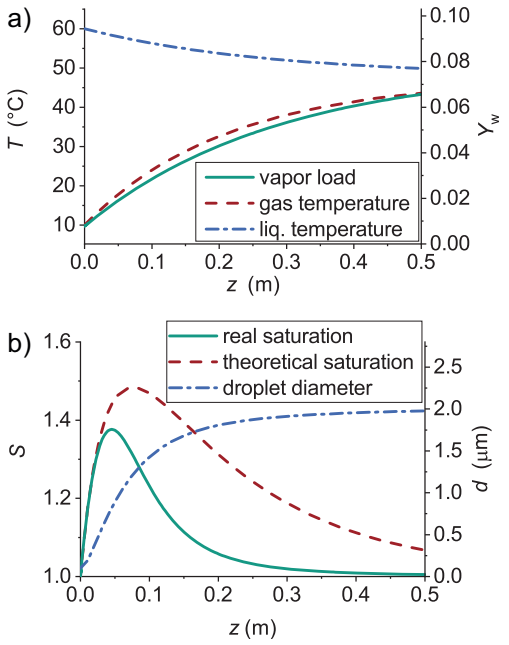

Figure 2. (a) Temperature (left axis) and water vapor load (right axis) versus column length. (b) The same plots for saturation (left axis) and aerosol droplet diameter (right axis). Results calculated with AerCoDe3.0 by using the input data provided in [11].

This gas is contacted with water at a temperature of $T^L = 60\,°C$. The liquid/gas ratio is defined as:

$$\tilde{m}^L := \frac{\dot{m}^L}{\dot{V}^G} \tag{2}$$

and has a value of $5\,\mathrm{kg\,m^{-3}}$ in this setup. As random packing for the column, plastic Pall rings with a size of 25 mm are chosen [22]. The resulting theoretical saturation curve has good conformity with the data of Heidenreich [11]. Additionally, the present calculations include heterogeneous nucleation and droplet growth with a number concentration of $c_N = 10^6\,\mathrm{cm^{-3}}$ monodisperse particles with an initial diameter of $d = 0.1\,\mu m$. Due to the fast rising saturation, the droplets grow fast in the first part of the device and reach 80 % of their end diameter at a column length of 0.15 m. The liquid temperature on the other hand is decreasing slower.

In this example, the equilibrium temperature of gas and liquid phase is 48 °C. After 0.15 m, the liquid has cooled down by 4.5 K, which corresponds to 37.5 % of the total temperature difference. At the end of the device, the water leaves with a temperature of 50 °C, i.e., 83 % of the total temperature drop. Keeping in mind this behavior, the challenge is to design a process, where the droplets grow enough to be separated easily, while the energy consumption due to the drop of liquid temperature and due to evaporation is kept minimal.

For different separators, Holzer [1] hints a logarithmic correlation between cut size of separated particles and energy consumption. A comparison of different particle separators shows that wet scrubbers can efficiently separate particles larger than 1 µm. The energy consumption of those scrubbers ranges from 0.2 to 1.5 kWh $(10^3\,\mathrm{m^3})^{-1}$ [23].

To assess different operation modes, a lower boundary for the thermal energy consumption of the condensation device can be defined. This is expressed as the sum of the energy for reheating the circulating scrubbing liquid and for heating additional fresh water to compensate evaporation:

$$E_{\mathrm{cond}} = \frac{\left(T^{\mathrm{L}}_{\mathrm{in}} - T^{\mathrm{L}}_{\mathrm{out}}\right) c^{\mathrm{L}} \dot{m}^{\mathrm{L}}_{\mathrm{out}} + \left(T^{\mathrm{L}}_{\mathrm{in}} - T^{\mathrm{G}}_{\mathrm{out}}\right) c^{\mathrm{L}} \left(\dot{m}^{\mathrm{L}}_{\mathrm{in}} - \dot{m}^{\mathrm{L}}_{\mathrm{out}}\right)}{\dot{V}_{\mathrm{G}}} \tag{3}$$

where the energy consumption of pumps and ventilators is neglected and, as a best-case scenario, the fresh water is assumed to be provided at gas outlet temperature. If the preconditioning process is operated as described above (basic data of Fig. 2), the energy consumption for the separation can be reduced from about 3 kWh $(10^3\ \mathrm{m}^3)^{-1}$ to less than 0.5 kWh $(10^3\ \mathrm{m}^3)^{-1}$ [23]. In this case, a packed-bed scrubber, which can be used to separate the grown droplets, replaces a Venturi scrubber, which separates the initial particles with a diameter of 0.1 µm. On the other hand, alone the thermal energy consumption of more than 60 kWh $(10^3\ \mathrm{m}^3)^{-1}$ (Eq. (3)) to reheat the trickling water is more than 20 times higher than the possible saved electrical energy of 2.5 kWh $(10^3\ \mathrm{m}^3)^{-1}$. To operate the process economically, this energy must be reduced.

As mentioned before, the main part of the droplet growth takes place in the first section of the column, while E_{cond} as a function of liquid temperature and evaporation is increasing over the whole device. Thus, cutting off the device, when a given droplet diameter d^* is reached, should significantly reduce the energy consumption. In Fig. 3, the droplet diameter is compared to the thermal energy effort for the first 0.25 m of the column. If a diameter of 1.2 µm is to be reached, it is sufficient to use a packing height of 0.075 m, which means an energy effort of 20 kWh $(10^3\ \mathrm{m}^3)^{-1}$.

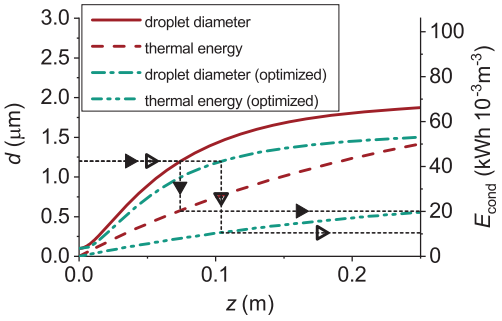

Figure 3. Comparison of droplet growth (left axis) and energy consumption (Eq. (3)) (right axis) for the initial parameters given in [11] (solid and dashed lines) and for optimized inlet parameters: $u^{\mathrm{G}} = 1\ \mathrm{m\,s^{-1}}$, $\tilde{m}^{\mathrm{L}} = 2.85\ \mathrm{kg\,m^{-3}}$, $T_{\mathrm{in}}{}^{\mathrm{L}} = 40\ ^{\circ}\mathrm{C}$ (dash-dotted lines).

Further parameters, which can be easily adjusted during process design, are inlet liquid temperature $T_{\mathrm{in}}{}^{\mathrm{L}}$, liquid/gas ratio $\tilde{m}^{\mathrm{L}}$, and gas velocity u^{G}. The influence of these input parameters on the maximum theoretical saturation $S_{\mathrm{th,max}}$, on the energy consumption (Eq. (3)), and on z^*, which represents the column length, needed to reach a droplet diameter of $d^* = 1.5$ µm, are evaluated by a parameter study, where the input parameters of [11] ($u^{\mathrm{G}} = 2.2\ \mathrm{m\,s^{-1}}$, $T_{\mathrm{in}}{}^{\mathrm{L}} = 60\ ^{\circ}\mathrm{C}$, $\tilde{m}^{\mathrm{L}} = 5\ \mathrm{kg\,m^{-3}}$) are considered as reference values for optimization.

Firstly, to investigate the influence of the single parameters, each of them is varied, while keeping constant the other two. The results are visualized in Fig. 4, where in each column the variation of one parameter is displayed. For all variations the three crucial parameters for the assessment of the process efficiency, $S_{\mathrm{th,max}}$, z^*, and E_{cond}, are displayed one above the other.

With lower gas velocity, and consequently reduced turbulence, the heat and mass transfer per liquid surface area is

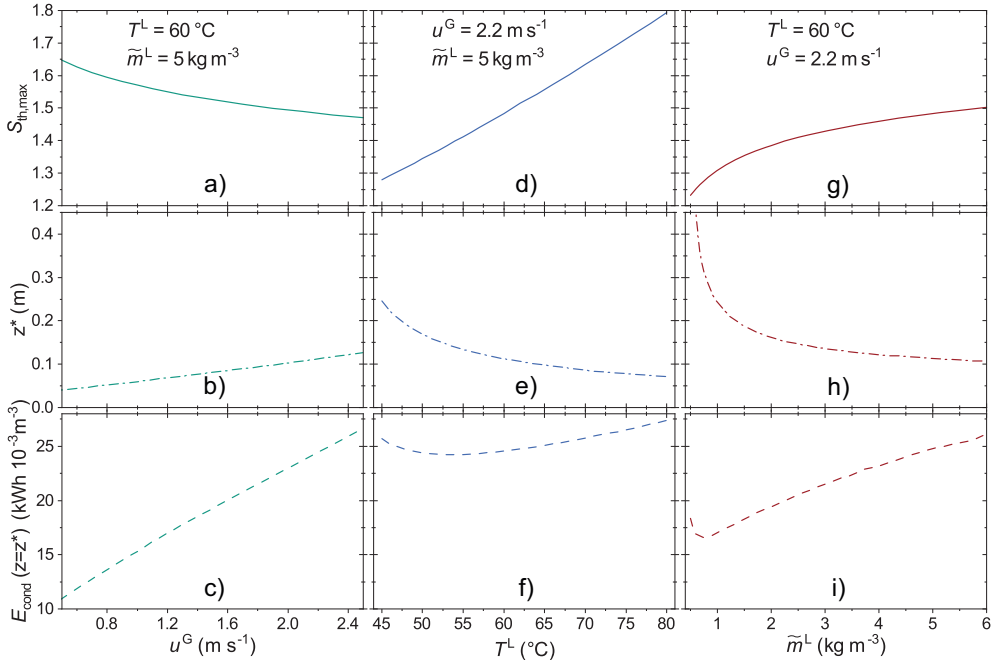

Figure 4. Maximum saturation (a, d, g), optimal packing height (b, e, h), and energy consumption (c, f, i) versus gas velocity (a, b, c), liquid temperature (d, e, f), and gas/liquid ratio (g, h, i), while generating droplets of 1.5 µm.

reduced, but again, as the gas flows slower, the residence time of the gas in the device increases. The latter is the dominant effect and allows shorter packing heights (Fig. 4b), since it leads to higher supersaturation (Fig. 4a). The reduced packing heights lead to a higher liquid outlet temperature and thus to a linear decrease of the energy effort (Fig. 4c). From the energetic point of view, it is best to have the gas flow as slow as possible. Consequently, the flow speed is downwards only limited by the allowed construction dimensions of the device.

The choice of lower liquid temperatures leads to lower supersaturation (Fig. 4d), but also helps to reduce the energy consumption (Fig. 4f), as the temperature gradient between gas and liquid is decreased. On the other hand, the enlargement of the column length (Fig. 4e), which is required for lower temperatures, increases the energy effort. For the given input, there is an optimal liquid inlet temperature for which the droplet growth is still great enough and the heat loss is minimal. It can be observed that the liquid inlet temperature has the largest effect on the maximum saturation (Fig. 4d), while it has only small impacts on the energy consumption (Fig. 4f).

With smaller liquid/gas ratio, the maximum saturation is reduced (Fig. 4g) and the devices must be constructed longer to increase the gas-liquid interfacial area (Fig. 4h). Furthermore, there is an operation point, where the tradeoff between reducing energy consumption by feeding less liquid mass and increasing energy consumption by longer contact time is optimal (Fig. 4i). When the liquid/gas ratio becomes too low, the necessary packing height z^* is steeply rising. This means that the outlet droplet diameter gets close to the maximum end diameter of droplet growth.

For constructional reasons, additional constraints on the range of the variables have to be considered. The liquid load of the device, which is defined as liquid volume flow per column cross-sectional area, should be kept between 10 and 40 $m\,h^{-1}$ and the gas velocity between 1 and 2 $m\,s^{-1}$. As stated above, it is optimal to choose the gas velocity as low as possible. For all consecutive calculations, u^G is set to 1 $m\,s^{-1}$. In the given range, it can be observed that, with decreasing liquid/gas ratio, the energy minimum is shifted to lower values and is reached for higher liquid temperatures (Fig. 5).

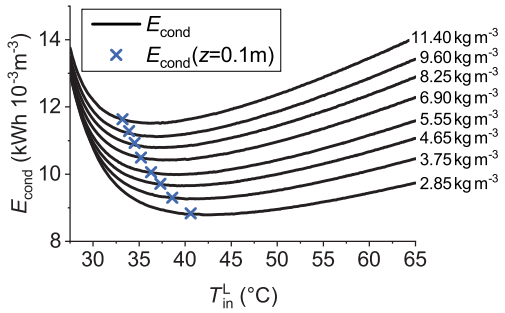

Figure 5. Thermal energy needed to reach a droplet diameter of 1.2 µm versus liquid inlet temperature for different values of liquid/gas ratio. Here, $c_N = 10^6\,cm^{-3}$, $T^G = 10\,°C$, and $u^G = 1\,m\,s^{-1}$.

With the given conditions for the particle-loaded gas, the absolute energy minimum is at a liquid inlet temperature of $T_{in}^{L} = 43\,°C$, with the minimum possible liquid/gas ratio of 2.85 $kg\,m^{-3}$. The demanded particle diameter of 1.2 µm is reached after 0.09 m, when the device consumes 8.8 kWh $(10^3\,m^3)^{-1}$ (Eq. (3)), as displayed in Fig. 3 (dash-dotted line). In this way, the optimal parameters for different simulation setups can be evaluated. Since the number concentration c_N of the initial particles has an essential impact on the final particle size, this parameter is varied between 10^5 and $10^7\,cm^{-3}$. Moreover, as a feed temperature of 10 °C would mean additional effort for cooling, cold gas at a temperature of 20 °C is considered.

Detailed tables for this parameter studies are provided online as Supporting Information. There, results for optimal packing heights and corresponding thermal energy effort can be found. If waste heat from other processes is available, it might be useful not to set the operation point to the minimum energy consumption, but to choose the minimum necessary liquid inlet temperature. Parameters for this case are also provided online.

Based on these results, two process sequences as preconditioning steps for fine dust separation are proposed (Fig. 6). Both use the energy of the exhaust gas to reheat the hot trickling water of a so-called short contact column. In the first stage, the gas is cooled down to the desired inlet temperature for the second stage, in which the cold gas is contacted with hot water. The dust particle growth takes place mainly in the second stage. To receive water for reheating at temperatures as high as possible, the gas cooling stage is divided into two consecutive packed columns. The first of them is trickled with water at a high temperature, to receive the needed heat for the consecutive step. The second column, which is operated with cooling water, supplies the main part of the cooling without additional refrigeration.

After the cooling step, a gas temperature of 20 °C is reached and shall be considered for the subsequent stage. The cool gas leaves the first stage saturated, with the fine dust particles already wetted. Subsequently, the gas is trickled with hot water in the short contact column in co-current flow. Here, heterogeneous condensation and droplet growth on the fine dust particles surface take place as described before. In both layouts, an original saturated exhaust gas at a temperature of 50 °C and loaded with $10^6\,cm^{-3}$ particles is assumed. To achieve a droplet diameter of d = 1.4 µm, the hot water from the first column can be directly used to trickle the short contact column (Fig. 6a).

The operation point with the lowest possible temperature for the short contact column is chosen (Tab. S6 in the Supporting Information). This means a higher energy demand, which, however, is covered completely by waste heat of the gas. The short contact column has a packing height of 0.5 m. It is operated with a liquid/gas ratio of 6.5 $kg\,m^{-3}$ and a liquid inlet temperature of 44 °C. This is sufficient to generate droplets larger than 1.4 µm for particle concentrations of $10^6\,cm^{-3}$, which can then be separated in a subsequent step. This last separation step is not part of the present work.

The second layout is used to generate droplets of 2 µm (Fig. 6b). In this case, a higher liquid inlet temperature is required for the short contact column. Therefore, the installation of a heat pump to shift the temperature of the waste heat to the desired level is suggested. The short contact column in this layout should be operated with minimum energy effort (Tab. S4).

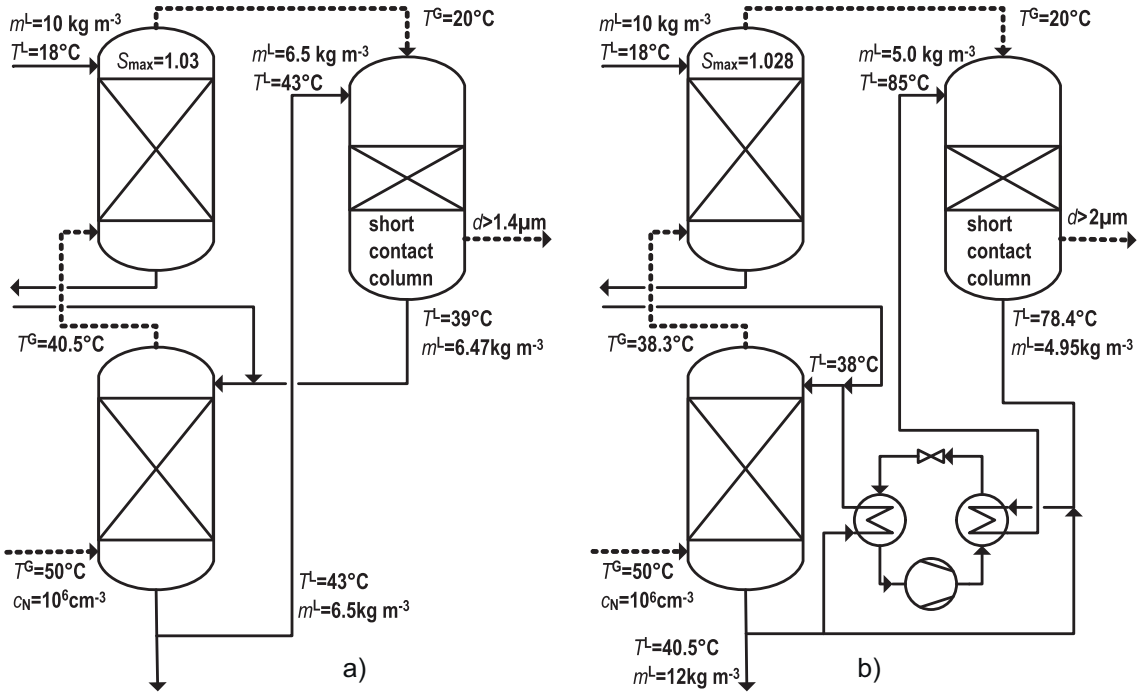

Figure 6. Process layouts for condensational particle growth: (a) direct waste heat usage and (b) heat pump usage, this last yielding a higher temperature and larger particle diameters.

For this purpose, a packing height of 0.1 m, a liquid temperature of 85 °C, and a liquid/gas ratio of 5.0 kg m^{-3} are chosen. This is sufficient to generate particles larger than 2.0 µm at a concentration of 10^6 cm^{-3}. For the heat pump, the operation with a temperature shift of 45 K to an upper temperature level of 85 °C yields a theoretical maximum coefficient of performance of COP_{max} = 8. Assuming a realistic COP of 4.5, the heat pump will consume less than 8.7 kWh $(10^3\ m^3)^{-1}$ electrical energy to provide the needed thermal energy of 39 kWh $(10^3\ m^3)^{-1}$ (Eq. (3)).

5 Conclusion

AerCoDe3.0 is a validated and reliable simulation tool to describe the droplet growth in packed columns. It is capable of describing any desired process sequence and can easily be adapted to specific waste gas conditions. In previous publications, the concept of condensational droplet growth was proved and layouts to generate droplets as large as possible were presented. In the present work, a further step is taken by studying the energy consumption of the devices and consequently providing solutions for energetically optimized process layouts.

It has been shown that thermal energy for reheating the scrubbing liquid is the main contribution to the energy effort, and that this can be reduced by choosing the packing height as small as possible, and by decreasing gas velocity, liquid/gas ratio, and liquid temperature. The lower limits of those reductions were calculated for various particle concentrations and the application limits of the method were pointed out. For a typical particle number concentration of 10^6 cm^{-3}, droplet diameters of 2 µm can be achieved with the proposed method. To generate larger droplets or to handle gases with particle concentrations of $c_N > 10^6$ cm^{-3}, the energy effort is too high to operate the process economically.

Acknowledgment

This research has been funded by the Federal Ministry for Economic Affairs and Energy of Germany in the frame of the project "Verbesserung der Energieeffizienz bei der Aerosolabscheidung, Teilvorhaben: Benetzbarkeit von Aerosolen und Ausarbeitung von Anlagekonzepten" (project no. 03ET1073B).

The authors have declared no conflict of interest.

Symbols used

c^L	[J kg^{-1}K^{-1}]	specific heat capacity of the liquid
c_N	[cm^{-3}]	number concentration of wettable particles or aerosol droplets
COP	[–]	coefficient of performance
d	[µm]	aerosol particle diameter
d^*	[µm]	desired droplet diameter for separation
E_{cond}	[kWh $(10^3\ m^3)^{-1}$]	thermal energy consumption of the condensation device
$\dot{m}$	[kg s^{-1}]	mass flow
$\tilde{m}^L$	[kg m^{-3}]	liquid/gas ratio
p_{sw}	[Pa]	vapor pressure of water

p_w	[Pa]	partial pressure of water
S	[–]	saturation ratio
S_{crit}	[–]	saturation ratio, critical value
S_{th}	[–]	theoretical saturation ratio without aerosol formation
T	[K]	temperature
u	[m s^{-1}]	velocity
$\dot{V}$	[m^{3}s^{-1}]	volume flow
Y_w	[kg kg^{-1}]	vapor load of the carrier gas
z	[m]	column length
z^*	[m]	optimized column length to reach d^*

Sub- and superscripts

G	gas phase
in	device inlet
L	liquid phase
max	maximum value
out	device outlet
th	theoretical value
w	water

References

[1] K. Holzer, *Chem. Ing. Tech.* **1979**, *51 (3)*, 200–207. DOI: https://doi.org/10.1002/cite.330510308

[2] F. Fahnoe, A. E. Lindroos, R. J. Abelson, *Ind. Eng. Chem.* **1951**, *43 (6)*, 1336–1346. DOI: https://doi.org/10.1021/ie50498a026

[3] P. J. Schauer, *Ind. Eng. Chem.* **1951**, *43 (7)*, 1532–1538. DOI: https://doi.org/10.1021/ie50499a022

[4] B. W. Lancaster, W. Strauss, *Ind. Eng. Chem. Fundam.* **1971**, *10 (3)*, 362–369. DOI: https://doi.org/10.1021/i160039a004

[5] T. Yoshida, Y. Kousaka, K. Okuyama, *Ind. Eng. Chem. Fundam.* **1976**, *15 (1)*, 37–41. DOI: https://doi.org/10.1021/i160057a007

[6] T. Yoshida, Y. Kousaka, K. Okuyama, F. Nomura, *J. Chem. Eng. Jpn.* **1978**, *11 (6)*, 469–475. DOI: https://doi.org/10.1252/jcej.11.469

[7] S. Calvert, in *Handbook of Air Pollution Technology* (Eds: S. Calvert, H. M. Englund), Wiley-Interscience, New York **1984**, 236.

[8] T. Johannessen, J. A. Christensen, O. Simonsen, H. Livbjerg, *Chem. Eng. Sci.* **1997**, *52 (15)*, 2541–2556. DOI: https://doi.org/10.1016/S0009-2509(97)00071-7

[9] S. Heidenreich, F. Ebert, *Chem. Eng. Process.* **1995**, *34 (3)*, 235–244. DOI: https://doi.org/10.1016/0255-2701(94)04009-5

[10] S. Heidenreich, U. Vogt, H. Büttner, F. Ebert, *Chem. Eng. Sci.* **2000**, *55 (15)*, 2895–2905. DOI: https://doi.org/10.1016/S0009-2509(99)00554-0

[11] S. Heidenreich, *Chem. Ing. Tech.* **2005**, *77 (1–2)*, 35–45. DOI: https://doi.org/10.1002/cite.200407059

[12] N. H. Fletcher, *J. Chem. Phys.* **1958**, *29 (3)*, 572–576. DOI: https://doi.org/10.1063/1.1744540

[13] M. Lazaridis, M. Kulmala, B. Z. Gorbunov, *J. Aerosol Sci.* **1992**, *23 (5)*, 457–466. DOI: https://doi.org/10.1016/0021-8502(92)90017-P

[14] W. C. Hinds, *Aerosol Technology: Properties, Behavior, and Measurement of Airborne Particles*, 1st ed., John Wiley & Sons, New York **1982**.

[15] A. Schenkel, K. Schaber, *J. Aerosol Sci.* **1995**, *26 (7)*, 1029–1039. DOI: https://doi.org/10.1016/0021-8502(95)00038-E

[16] L. Brachert, *Charakterisierung von Schwefelsäureaerosolen in technischen Prozessen*, 1st ed., Verfahrenstechnik, Verlag Dr. Hut, München **2014**.

[17] J. Körber, K. Schaber, R. Ehrig, P. Deuflhard, *J. Aerosol Sci.* **1998**, *29*, S579–S580. DOI: https://doi.org/10.1016/S0021-8502(98)00363-2

[18] R. Ehrig, O. Ofenloch, K. Schaber, P. Deuflhard, *Chem. Eng. Sci.* **2002**, *57 (7)*, 1151–1163. DOI: https://doi.org/10.1016/S0009-2509(02)00015-5

[19] O. Ofenloch, *Entstehung und Verhalten von Aerosolen in Gaswaschanlagen*, 1st ed., Fortschrittberichte VDI, Series 3, Vol. 832, VDI-Verlag, Düsseldorf **2005**.

[20] A. Wix, *Theoretische und experimentelle Untersuchungen zur homogenen und heterogenen Nukleation bei der Säureabsorption in Gas-Flüssigkeitskontaktapparaten*, 1st ed., Fortschrittberichte VDI, Series 3, Vol. 894, VDI-Verlag, Düsseldorf **2008**.

[21] H. Gretscher, *Entstehung von Aerosolen durch heterogene Keimbildung bei der Absorption und Kondensation*, Fortschrittberichte VDI, Series 3, Vol. 650, VDI-Verlag, Düsseldorf **2000**.

[22] R. Billet, M. Schultes, *Chem. Eng. Technol.* **1993**, *16 (1)*, 1–9. DOI: https://doi.org/10.1002/ceat.270160102

[23] E. Schmidt, in *Ullmann's Encyclopedia of Industrial Chemistry* (Ed: B. Elvers), Wiley-VCH, Weinheim **2008**, 637–673. https://onlinelibrary.wiley.com/doi/pdf/10.1002/14356007.b02_13.pub2

